Title

CORRELATION OF THERMO-MECHANICALLY VARIED MICROSTRUCTURES WITH SUPERCONDUCTING PROPERTIES OF Nb3Sn PROCESSED BY A NEW POWDER METALLURGY TECHNIQUE

Author

Babu, B. Naga Prakash.

Publication Date

1971-12-01

LBL-437
c.1

CORRELATION OF THERMO-MECHANICALLY VARIED MICROSTRUCTURES WITH SUPERCONDUCTING PROPERTIES OF Nb_3Sn PROCESSED BY A NEW POWDER METALLURGY TECHNIQUE

B. Naga Prakash Babu
(M.S. thesis)

December 1971

AEC Contract No. W-7405-eng-48

LBL-437
c.1

DISCLAIMER

Table of Contents

CORRELATION OF THERMO-MECHANICALLY VARIED MICROSTRUCTURES WITH SUPERCONDUCTING PROPERTIES OF Nb_3Sn PROCESSED BY A NEW POWDER METALLURGY TECHNIQUE

B. Naga Prakash Babu

Inorganic Materials Research Division, Lawrence Berkeley Laboratory and Department of Materials Science and Engineering, College of Engineering; University of California, Berkeley, California

ABSTRACT

A flexible, stable Nb_3Sn composite was fabricated by a new powder metallurgy technique. Related studies and optimization of parameters in each step of the fabrication were made. The dependence of transition temperature on microstructural aspects was considered; an explanation was offered for the lowering of T_c at higher reaction temperatures and the effect of reaction time is discussed. Short sample tests were made and current densities at d.c. fields upto 80 KG were measured; flexibility and stability were tested. Finally, an evaluation of all the process parameters was made and an optimum process schedule was developed. The T_c for most samples ranged from 18.1 to 18.45°K. The current density in the Nb_3Sn phase was around 2.7×10^5 Amps/cm^2 at 80 KG.

I. INTRODUCTION

Starting with the epoch-making discovery of Nb_3Sn as a high field superconductor by Kunzler, et al.[1] 1961, many investigators have explored different ways of fabricating flexible tapes and wires of Nb_3Sn to circumvent its inherent brittleness. In this direction, RCA ribbon[2] was made by vapor deposition process and G. E. tape[3] was made by a diffusion process. The basic objective in every approach has been to obtain a thin sandwich of Nb_3Sn between stabilizing copper layers, so that the composite as a whole is flexible. The superconducting layer near the neutral axis of the composite suffers little deterioration in properties when the tape is bent. The new powder metallurgy technique[4] developed in this laboratory involves making such a flexible composite having 2-4 microns thick superconducting filaments.

The fabrication involved, powder rolling of porous niobium strip followed by sintering into a ductile spongy structure, which was then infiltrated with tin. The two-phase network so created was quite versatile as it was possible to obtain a wide variety of microstructures by variations in the degree of cold work prior to the diffusion heat treatment, and in time and temperature of the heat treatment. The work reported herein provided a correlation of these thermo-mechanically varied microstructures with the superconducting properties of Nb_3Sn. The objective was to arrive at an optimum microstructure.

Efforts were made to arrive at optimum parameters, such as powder size, roll gap, sintering temperature, time, and environment, infiltration time and temperature, and heat treatment time, temperature, and environment. Transition temperatures were measured resistively. Some fascinating observations were made of the lowering of T_c of Nb_3Sn by the higher temperature treatments. Critical current measurements could be made only on a few representative samples. These were typical short sample characteristics obtained using steady-field techniques. Similar data obtained by pulsed field techniques on the same samples are presented by T. Garret in his thesis.[5] Tentative inferences on the optimum degree of cold work, stability and flexibility were made.

The samples were examined metallographically. The phases were usually identified by their characteristic colors[6] obtained by anodising. The identifications were checked in a few samples by x-ray diffraction. The Nb_3Sn composition was determined with the electron beam microprobe. The scanning electron microscope was used to study the different powders; powder classification was done using the Allen-Bradley Sonic Sifter.

II. IMPORTANCE OF MICROSTRUCTURE

The transition temperature T_c and the thermodynamic critical field $H_c(T)$ are primary properties defined by the electron structure, the phonon spectrum, and the electron-phonon interaction. Structural defects like dislocations, grain boundaries or intrinsic point defects are not expected to affect these properties appreciably.[7] An understanding of what determines the T_c of a superconductor is still very limited. According to BCS theory, T_c increases quite sensitively with the product NV, N being the density of states at the Fermi surface and V, the electron-electron interaction parameter. Although N can be derived, V remains underivable unless T_c is known.[8] However, T_c as observed in the foregoing studies, is affected by stoichiometry and order.

The GLAG theory throws considerable light on the critical fields of type II superconductors; according to this concept, $H_{c2} = \sqrt{2}\, KH_c$; K, the Ginzburg-Landau parameter = λ/ξ i.e., penetration depth of the flux/coherence length. K is also given as K_ℓ ($\approx N^{1/2}\, \ell^{-1}$, l-electron mean free path) + K_0 = ($\approx T_c N^{3/2}$). Nb_3Sn has a very high N, having the intrinsic part $K_0 \gg$ extrinsic part K_ℓ. Hake[9] is of the opinion that H_{c2} of Nb_3Sn can be made as high as 830 KG, if ℓ is made small, that is when K_ℓ also becomes large. The major effect of metallurgical structure is through the effect of defects on ℓ, and hence on K. Dislocations have a pronounced effect - their strain fields and the stacking faults scatter the conduction electrons and reduce

the mean free path - thereby increase K. But in case of Nb_3Sn, the dislocation effect is questionable; H_{c2} can however be enhanced by obtaining Nb_3Sn in the form of thin films and by having extremely fine grains.

Trauble and Essmann[10,11] have shown by their exciting series of experiments, that critical currents in the mixed state (between H_{c1} and H_{c2}) are controlled by the interaction between the metallurgical and magnetic microstructures. With the increase in externally applied magnetic field, the flux penetration increases beginning at H_{c1} and is complete at H_{c2}. The flux filaments driven by the Lorentz force, $\bar{F}_L = \bar{J} \times \bar{H}$, move with a velocity V, against the pinning force F_p, consuming a power $P = nF_pV$ (n = number of flux filaments), which is evidenced as electrical resistance, with the consequent appearance of a voltage. In regard to the pinning force, the model developed by Bean[12] and that developed by London[13] state that a normal particle in the matrix or adjacent to the surface of the superconductor will provide stronger pinning than a superconducting particle, and an oxide particle or void would provide still stronger pinning.

For the Nb-Nb_3Sn-Sn composite considered in the foregoing studies, pinning by grain boundaries[14] and surface pinning can be considered. Nb_3Sn filament sandwiched between normal niobium and tin or in niobium matrix only will have highly pinning surfaces. For best anisotropy and so for extremely high J_c, a multiple layer sample of alternating superconductor and oxide is suggested. In the composite considered

here, an oxide of niobium at the interface of Nb and Nb_3Sn should be an excellent pinning source.

III. PROCESSING OF THE STRIP AND RELATED STUDIES

The processing of the composite involved selection of powder fraction, powder rolling, sintering, infiltration, cold working and diffusion heat treatment.

A. Powder and Powder Classification

Wah Chang -270 mesh* Niobium Powder of 99.92% purity was used. A sieve analysis showed that this powder was practically all -325 mesh, and that 70% of it was -400 mesh. Micro-sieve analysis of -400 mesh fraction gave almost equal percentages of -400 + 500, -500 + 750, -750 + 1000 and -1000 mesh fractions.

The cross-section of a strip made with -270 mesh powder showed a non-uniform porosity except at the edges, where there was a larger porosity. The edges are loosely bonded when the strip is rolled from powder (See Figs. 1(a) and (b)). The uneven distribution of pores is attributed to the wide distribution in particle size. It was also found that the porosity would vary with different lots of powder for the same rolling parameters. The particle size distribution was found to be different. To obtain a rigid control over microstructure, an accurately graded powder fraction was required.

Sub-sieve (-400 mesh) classification of powder was done using an Allen-Bradley sonic sifter using electro-formed nickel mesh sieves - operating on the principle of elutriation by sonic vibration. Strips

---

* U.S. Tyler Standard Sieve No.

rolled out of the various fractions, with the same roll gap and roll speed, were identically sintered and infiltrated. Studying the microstructures, shown in Figs. 1 to 4, it appears that the porosity - increased with finer powder sizes, but when the powder was too fine, e.g., -10μ (= -1000 mesh), the pore size too small for good tin infiltration and some of the pores were unconnected. An optimum volume fraction, with an extremely fine distribution of pores, appeared to be in -20 + 10μ (= -750 + 1000 mesh) range.

A scanning electron microscope study of various fractions showed that the particles were angular and highly irregular in shape. The particle shape contributed to the good green strength of the rolled strip. The micrographs of the sharply graded fractions showed the uniformity of particle size (Figs. 6(a), (b) and (c)).

B. Powder Rolling

The rolls[15] used were of 2 inch diameter, the axes were in the horizontal plane. The powder feeding was by gravity through a lucite hopper. The rolling mill had a stepless variable speed motor drive. Grooves 1/8 in. deep were cut in the rolls, leaving a 1/4 in. wide rolling surface between the grooves. The grooves prevented the lateral spread of the powder and provided better edges on the rolled strip. To confine the powder within the grooves, two lucite side retainers of 1/8 in. thick were machined to straddle the rolls. They fitted in the grooves and rested on the reduced rolls. The retainers were assembled with 1/4 in. lucite spacers, 2 in. apart. They rested on

the rolls. A lucite hopper was added to this assembly. It had an adjustable slide to meter the powder flow and to maintain a constant powder head. A photograph of the rolling mill assembly is given in Fig. 7(a).

A roll gap of 0.012 in. was used in all experiments. There appeared to be a maximum roll gap, above which compaction could not be accomplished. For finer powders, which give fairly good green strength, 0.012 in. seems to be an optimum value. Also with this gap, adequate porosity was obtained in case of -270 mesh, and -750 + 1000 fraction powders. A roll speed of 5rpm at which the strip emerges at $2\frac{1}{2}$ feet per minute was used throughout.

C. Sintering of Green Strip

The green strip emerging out of the rolls is strong enough to support a few feet of its own weight. The surface appearance and the green strength vary with different powder fractions for the same roll gap and roll speed.

Samples 3 inches long of the green strip were mounted vertically on a tantalum holder. Sintering, infiltration and heat treatment were all done in an ABAR vacuum furnace. The heating element was a split tungsten mesh cylinder, 1 in. in diameter and $2\frac{1}{2}$ in. long. A maximum temperature of 2350°C, and vacuum 2×10^{-5} torr or better could be obtained. The tantalum holder with the samples was held by a stainless steel rod passing into the furnace top through a vacuum seal.

Sintering conditions were 2225°C for 3 minutes in a vacuum $< 4 \times 10^{-5}$ torr, with a preheat for a few minutes at 1900°C. Sintering time was not found to be critical at this temperature. There was no detectable change in porosity when the time was increased to 6 minutes, and the ductility of the sintered strip was practically the same. However, much longer times drastically decreased the porosity. It was found that 1/2 minute holding at 2350°C (close to the melting point of niobium) produced the same porosity and ductility that were obtained at 2225°C for 3 minutes. This would mean that on a continuous fabrication system, the length of the heating element could be reduced to 15 in. for a strip emerging at 30 in. per minute from the rolls. The temperature was measured using W-5 % Re Vs W-26 % Re thermocouple. A check by a radiation pyrometer was also made, as well as temperature checks upto 1700°C made with a Pt-Pt. 10% Rh thermocouple.

In the ABAR furnace, strips of less than $2\frac{1}{2}$ in. could be sintered. The length was limited by the length of the heating element. To make strips 8-10 in. long, which were required for short sample testing in steady-fields, a 7 in. long extension sleeve was installed on top of the furnace. The long strip was passed through the sleeve, with the lower $2\frac{1}{2}$ in. in the element. The strip was lowered vertically at the rate of 1 in./minute, so that the entire strip was sintered uniformly in about 3 minutes.

D. Infiltration

The quench pot attachment facility in the furnace was used for holding a 10 in. long quartz tube, in which tin bath was held in a graphite crucible heated externally. The furnace set up is shown in Fig. 7(b). The sintered sample, when cooled was lowered into a molten tin pool stabilized at 650°C. When dipped in the pool, tin flowed into the interconnected network of pores by capillary action. Temperatures lower than 550°C resulted in partial or no infiltration. Temperatures higher than 650°C and longer times at this temperature led to the formation of Nb_6Sn_5. The formation of this hard brittle intermediate phase had to be avoided, at least to the extent no significant amount of this formed at the interface. Otherwise the rollability of the infiltrated strip would be very badly impaired. 1-2 minutes at 625-650°C was found to be the optimum time. The infiltration and diffusion heat treatments can be carried out simultaneously in the tin bath, but this precludes mechanical working of the strip prior to the heat treatment.

E. Cold Working of Infiltrated Strip

The motive for cold working the strip prior to the diffusion reaction was to obtain elongated tin filaments in the microstructure, which upon alloying would form fine Nb_3Sn filaments. With proper infiltration, it was found that the rollability of the strip was fairly good. The problem encountered was the edge-cracking. After about 50% reduction, achieved in 3-4 passes, the edges developed tiny cracks, which, unless filed or trimmed at this stage would propagate and break

the strip. The strip could be rolled from 16 mils to 1 mil thickness with about 95% reduction. This was accomplished in slow stages, with intermediate trimming of the edge cracks.

It was found that some tin from the pores had squeezed out during cold reduction because of the morphology of the strip, and the difference in flow stresses of niobium and tin. There was a progressive reduction in the volume fraction of tin with increasing mechanical reduction, as can be noted in the photo micrographs, Figs. 5(a) to (e). A correlation of the amount of tin lost with the degree of cold work is shown in Fig. 8. The roll pressure was another important parameter. The higher the roll pressure, the greater was the amount of tin squeezing out for the same reduction. The micrograph of the 95% reduced sample (Fig. 5(d)) shows cavities in niobium; when severely reduced under relatively high roll pressure, the cavities closed, squeezing out tin, but when the pressure was released, the cavities opened up elastically.

So, rolling beyond 85 to 90% is not recommended. Extreme-useful reductions could possibly be accomplished if the strip is worked at a temperature below the recrystallisation temperature of tin.

F. Diffusion Heat Treatment

The diffusion heat treatment was carried out on short samples at temperatures varying from 800° to 1700°C and for times varying from a few minutes up to two hours. The microstructures of one, 'as infiltrated', sample treated at 1000°C for 16 hours, are given in Figs. 9(a) and (b). The heat treatments were done either in vacuum, in inert atmosphere,

or in a molten tin bath. Vacuum heat treatment had a deleterious effect on the surface of the sample. The tin evaporated from the surface, leaving the pores open. The vapor pressure of tin is 10^{-4} torr at 1000°C, increasing to 2 torr at 1700°C. Heat treating in an inert atmosphere minimized vaporization. However, efforts to get a ductile sample by sintering in He or Argon, could not be materialized but there is no reason why this should not be possible if an ultra pure inert gas is used.

It is doubly advantageous to do the heat treatment in a tin bath as this can reduce the steps in the fabrication process, because a final tin dip is essential to facilitate soldering of the strip. A heavy coating of tin adds to the stability of the composite as a superconductor, and moreover allows the composite to be bent without breaking.

IV. EXPERIMENTAL METHODS

A. Metallography

The anodization method described by Picklesimer[16] was used for delineating the phases present in the samples. The samples were prepared for anodisation by mounting in a mounting powder, abrading on silicon carbide papers down to 600 grit, and micropolishing using 0.05μ alumina as a thick slurry, the liquid being composed of 10 cc of 10% NaOH, 5 cc of H_2O_2 and 140 cc of distilled water. The samples were then anodised at 27 volts for 6 minutes, using a solution of 240 cc ethyl alchohol, 40 cc of distilled water, 20 cc of phosphoric acid, 40 cc lactic acid, 80 cc glycerine and 8 gm ciric acid kept at room temperature. The anodising conditions were similar to the ones used by Enstram et al;[17] so the characteristic colors were well standardised: Nb_3Sn always anodised dark blue or violet, Nb light blue, Sn yellow, Nb_6Sn_5 as reddish brown color.

Volume fraction analysis of Sn and Nb_3Sn in various samples was tried by a two-dimensional systematic point count method. However, this was too tedious, an improvised method was adopted. This consisted in weighing the photomicrograph, then cutting out the part corresponding to the phase in question and weighing that part. The weight ratios would give the volume fraction accurately.

B. Electron Probe Microanalysis

Electron probe microanalysis was performed on a few samples. The characteristic x-ray intensities of NbKα and SnLα from Nb_3Sn were compared with those from the unreacted niobium and tin phases also in the

same anodised sample, thereby avoiding the errors associated with using different samples. Variations in the anodisation could affect the counts from niobium in particular,[18] but the error involved was considered negligible.[18] The ratios were corrected for absorption effect as per the procedure laid out in NASA PUB TND - 2984. The purpose of the analysis was to determine the composition gradient, if any, in Nb_3Sn, as Nb_3Sn is known to have tin content varying from 17.5 at.% to 26 at.%.

The 'as infiltrated' sample heat treated for 16 hours at 1000°C, containing about 80% Nb_3Sn by volume, was used for a broad analysis. A volume fraction of 24.2% Sn is required to convert the niobium into Nb_3Sn of 25 at.% Sn. A typical -270 mesh sample cross-section showed an average volume fraction of about 21% in the center, while at the extreme edges, the volume fraction was about 33-34%. Thus after 16 hours of reaction, as shown in Figs 9(a) and (b), the central portion was predominantly Nb and Nb_3Sn, with very little Sn, while at the edges, there was Sn and Nb_3Sn, with very little Nb.

Microprobe analysis was also made on specimens Nos. JC-3 (L.S.* in Fig. 12 and JC-4 (C.S.** in Fig. 13a). (The cross sections of specimens, Nos. JC-1 and JC-2 are given in Figs. 10 and 11.) The phases were so thin in these samples.that the scanning had to be done in 0.5 micron step. It was confirmed that at portions where there was Nb-Nb_3Sn two phase equilibrium there was no compositional gradation. The composition was

---

* Longitudinal Section

** Cross Section

estimated to be around 17 to 18 at.% Sn, the stoichiometry referred to as Nb_4Sn in the earlier literature.[5,19] But in regions where Sn was present with Nb_3Sn (with or without niobium), there was the expected gradation in Nb_3Sn from about 18 at.% Sn to 26 at.% Sn. Also at the tin rich interface in samples JC-2 and JC-3, because of their comparatively slower cooling rates, a thin layer of the order of 0.5 micron of Nb_3Sn was observed. These findings were in compliance with the phase diagram given in Fig. 14.[18]

C. X-Ray Methods

Filings from the rolled and reacted samples were used for x-ray analysis on a diffractometer using CuKα radiation. The analysis was limited to phase identification. The analysis was done only on samples JC-2 and JC-4. The presence of Nb_6Sn_5 was found in both samples.

D. Transition Temperature Measurements

Temperature was measured in the cryogenic range by means of a germanium resistance thermometer calibrated to within ± 0.1°K (Texas Instruments Model 106) over the temperature interval from 4.2° to 40°K. The probe used was wired for two samples and it was a four point probe - a schematic of the circuitry is given in Fig. 15. The probe consisted of a copper block with two germanium thermometers on one side and the pressure contacts for mounting the sample on the other side. A copper cylinder cap was used to cover the copper block to avoid sharp thermal gradients. The probe with the samples was lowered into a long-neck liquid helium Dewar. A temperature gradient in its neck over the liquid

He level was used as a means for obtaining different sample temperatures. The probe was held for about 10-15 minutes until thermal equilibrium was obtained in the probe. Vertical movement of the probe produced the desired temperature variation. A current of one milliampere was passed through the sample, and the voltage across the sample was measured with a Nonovoltmeter (Astrodata Model 121 RZ). A current of 10 micro-amperes was passed through the Ge thermister. Both the voltage across the sample and the resistance of the thermometer were suitably amplified, and the signals were recorded simultaneously on an x-y recorder. The resistance transition was taken as the temperature at which signal became zero (within the sensitivity of the instrumentation). The thermister resistance at which this happened was converted into the temperature using the supplied calibration data. The width of the transition was defined as the temperature difference between 10% and 90% of the total voltage signal recorded in the normal state. The critical temperature data obtained are recorded in Fig. 16 and a discus sion is given in Chap. V., Sec. A.

E. Current Density Measurements

Current density measurements were made in the Superconductivity Laboratory (in Bldg. 64 - LBL). Two magnets in series with a total capacity of 90 KG were used, each being 4 in. in diameter, $2\frac{1}{2}$ in. long solenoid wound of 0.065 in. twisted cryomagnetics wire. The 7 in. long infiltrated strip obtained as described in Chap. III, Sec. C, was rolled down to the desired thickness and then coiled to a 1 in. diameter before reacting (by dipping into the tin bath heated to the reaction temperature).

Table I. Case History of the Samples, Prepared for Current Density Measurements.

Sample	Designation	Powder Mesh Size	Mechanical Reduction %	Specimen C.S.Area	Length inches	Vol. Fraction of Nb_3Sn %
JC-1	SP 710303	-270	50	.086"×.008"	12	≈ 5
JC-2	SP 710315	-270	75	.055"×.004"	8	≈ 11
JC-3	SP 710422-A	-750 + 1000	75	.060"×.004"	4.2	≈ 13
JC-4	SP 710422-B	-750 + 1000	90	.050"×.001"	-	≈ 22

Note: All Samples: Roll gap: 0.012 in. , roll speed: 5rpm
Sintering: 6 minutes at 2225°C.
Infiltration: I minute at 600°C.
Heat Treatment in tin bath: ≈ 2 minutes at 950°C.

The "short sample" coil so obtained was slipped on a 1 in. shaft mounted on a 3/4 in. diameter rod, which was then inserted into the center of the solenoid. Voltage connections were made close to the ends of the sample winding and were brought to the top of the Dewar. The voltage across the sample was measured with a chopper amplifier, which gave a maximum sensitivity of 1 microvolt per division on the multichannel recorder. Currents in the magnet and in the sample were monitored by series shunts and a field signal was obtained from a bismuth probe mounted on the sample holder. All these signals were recorded continuously. The resistivity was computed from the cross-sectional area of the superconductor, the length of the sample and the current and voltage.

High resistivities are undesirable. The resistivity of Copper at 4.2°K is 2×10^{-8} Ohm-cm. To avoid excessive resistive heat generation, a 'design-maximum' current density for a superconductor should be determined at an arbitrary resistivity, such as $\rho = 10^{-12}$ Ohm-cm.[20] So, in the short sample characteristic given in Fig. 18, the data points of constant resistivity are plotted. The points were obtained from the resistivity data given in Fig. 17. The case history of the samples used for these measurements is given in Table I.

The pulsed field measurements[5] made on the sample JC-2 show that the values agree quite well with the steady-field values when the magnetic field rise time is long enough, or when the rate of field change dH/dt is very small. This is the case when the field is at the peak. Also in this method, electrical 'noise' limits the sensitivity to which the onset of resistive field can be measured.[21]

V. EXPERIMENTAL RESULTS AND DISCUSSION

A. Critical Temperature Measurements

T_c values between 18.1°K and 18.45°K were obtained for most of the samples tested. Considering the very short times (1-3 minutes) of heat treatments, such high T_c values suggest that the A-15 phase is formed extremely readily. Also, the observation that Nb_3Sn of 18 at.% Sn had as high a T_c as the stoichiometric Nb_3Sn is not in agreement with some reports,[22,23] that Nb rich Nb_3Sn has a low T_c, but is analogus to the results of Reed et al.[19] and Courtney et al.[24]

It is stated[25] that high transition temperatures such as 18.1° to 18.3°K for Nb_3Sn can only be obtained by an ordering formation at optimum temperatures between 950° and 1000°C, but the present investigation showed that the T_c was fairly insensitive to temperatures between 900° and 1300°C when the time of heat treatment was limited to one hour. The T_c was also insensitive to the degree of cold work prior to the diffusion reaction, although cold work assisted in the formation of Nb_3Sn at lower temperatures such as 800-850°C. This supports the observation of Charlesworth et al.[18] While the 'as infiltrated' and reacted sample did not show any Nb_3Sn, the 50%, 75%, 85%, 95% reduced and reacted samples gave fairly high T_c values (17-6° to 17.9°K),

At higher temperatures (> 1400°C), for short times of heat treatment, very broad transitions were observed - transition width of about 9.5°K was observed. When the heat treatment time was limited to a few minutes, the start of transition was at 18.2°K, and complete transition occurred at 8.7°K - the T_c of niobium. It appears that if the heat

treatment time at high temperatures can be kept infinitesimally small, the T_c can be held at 18.2°K.

All the tin was converted into Nb_3Sn at 1000°C, before the sample was taken to higher temperatures in vacuum, lest tin should evaporate rapidly at these temperatures. A sample thus heat treated at 1700°C for one hour showed a small ΔT_c but had a T_c = 8.7°K and was ductile, suggesting that the strip could be just niobium. Another sample similarly heat treated but in an inert atmosphere gave a T_c = 6.7°K, with a small ΔT_c and the sample was brittle.

For longer heat treatment times e.g., an hour, broader transition widths were observed even at 1400°C. For much longer periods of heat treatment large ΔT_c were observed even at 1300°C. However, when the environment was an inert atmosphere, the degradation in T_c with the time of heat treatment was hindered at these temperatures.

Weight measurements of the samples were made prior to and after the heat treatment. Large weight losses were observed in samples treated in vacuum at temperatures > 1400°C, suggesting that the tin was volatalising from the Nb_3Sn lattice. The total loss of tin, observed in some samples had made them ductile. In inert atmosphere, tin had less tendency to volatalise.

These findings are in agreement with the observations of Courtney et al.,[24] who correlate the decreases in transition temperature with the deviations from stoichiometry, with the decrease in the lattice parameter and with the increase in tin loss. They conclude that the A chain in the A_3B structure must be preserved both in continuity and direction for high T_c.

B. Current Density Measurements

Critical currents, characteristic of Nb_3Sn were measured. At 80 KG, for sample JC-2, the current density in Nb_3Sn phase was $\sim 2.7 \times 10^{-5}$ Amps/cm^2 at a resistivity = 10^{-10} Ohm-cm. At 150 KG, as measured by pulse field technique, the current density was $\sim 6.5 \times 10^{4}$ Amps/cm^2 at a $\rho = 10^{-8}$ Ohm-cm. The details pertaining to the samples prepared for current density measurements are given in Table I. The resistivity data obtained on sample JC-3 are given in Fig. 17. The slope of the lines defined the breadth of the mixed state at various fields. The current densities at two resistivities 10^{-12} and 10^{-10} Ohm-cms for different fields obtained from this figure were plotted in Fig. 18 giving the conventional short sample characteristic. Sample JC-1 (C.S in Fig. 10) was prepared in the same way as JC-2 (C.S in Fig. 11) but had only 50% deformation prior to the reaction. It had lower current densities than the sample JC-2. This might have been the result of the less filamentary nature of Nb_3Sn in this sample.

The above samples were made by coiling and then reacting. They were mounted on the sample with great care taken not to disturb the preform, lest the Nb_3Sn filaments break. Sample JC-2 was tested in this way. Later, the sample was unsoldered from the contacts, uncoiled and was then reverse recoiled and was again mounted and tested. The current densities remained practically the same, suggesting that the superconducting helix could sustain such coiling and uncoiling, at least to 1 in. diameter with no deterioration in superconducting properties.

VI. GENERAL OBSERVATIONS AND CONCLUSIONS

A. Flexibility

The flexibility of the strip was dependent on the thickness of the superconducting filament. There was a critical thickness beyond which the strip would break if bent into 1 in. diameter; this was around 4-6 microns. Obviously, there was no point reacting any sample for longer periods so as to obtain larger volume fraction of Nb_3Sn as the thickness of the filaments would have been greater than the critical size. It was found that for good flexibility, 3 minutes was the maximum time of reaction. So, the only way to enhance the volume fraction was to increase the reaction surface. This was done by elongating the tin into filamentary form by mechanical reduction, although this resulted in some tin squeezing out. Thus, for 2 minutes of reaction, the volume fraction of Nb_3Sn in a 50% deformed sample was about 5-6%, while in 75% reduced sample, it was 11-12%, and in 85% it was about 25-30%. Thus for flexibility, the optimum reduction was around 85% and the reaction time was 2 to 3 minutes.

B. Stability

Because of its high pinning strength, Nb_3Sn is intrinsically very unstable.[26] As the magnetic field is increased, closed loops of current are formed. They are generally unstable, and may suddenly decay with evolution of heat. This rapid decay is known as flux jump and may cause a local rise in temperature sufficient to change the superconductor to the resistive state. The instability is partially overcome by improving

the thermal environment within the coil, and by bonding the superconductor to a normal metal to provide a temporary alternative current path. In the Nb-Nb_3Sn-Sn three phase composite, in the event of a hot spot, Nb, with a normal state resistivity at 4.2°K, $\rho_n = 5 \times 10^{-6}$ Ohm-cm and Sn with $\rho_n = 10^{-6}$ Ohm-cm[27] (compared to the ρ_n of $Nb_3Sn = 10^{-5}$ Ohm-cm[28]) will stabilize the Nb_3Sn phase. The combination of tin and niobium carry the same current with less voltage drop than normal Nb_3Sn. So the current density of the Nb_3Sn will decrease when the Nb_3Sn resistivity in the mixed state rises above the resistivity of the Nb-Sn combination. Thus, a good tin coating on the strip enhances the stability as well as the mechanical properties.

C. Other Optimum Parameters

Old and Macphail[29] have shown that the Nb_3Sn forms partly by diffusion and partly by a solution-deposition mechanism. The latter mechanism is more dominant at higher temperatures, thereby causing a slower growth rate. If the totally diffusion controlled reaction were to follow a $\sqrt{t}$ law i.e., $x = Kt^{0.5}$, x being the layer thickness after a time t. A combination of the two mechanisms modifies this equation to $x = Kt^{0.36}$, in the temperature range of 950° to 1150°C. Since the activation energy of the solution-deposition process is low, it is hard to eliminate its participation. The best way is to minimize the amount of tin. This leads to improved uniformity of the Nb_3Sn layers.[29] The cold work prior to the reaction made this possible by elongating the tin, and enhancing the surface area. Also, as observed in Chap. V, Sec. B, Nb_3Sn formed at lower temperatures such as 800°-850°C, when

assisted by the prior cold work. At 850°C, the diffusion mechanism following the usual equation $x^2 = 2\,Dt$ ($D \sim 10^{-10}$ cm^2/sec at 950°C for Nb_3Sn) is most likely to predominate.

Higher degree of cold work, low reaction temperature such as 850°C, and very short reaction time (2-3 minutes) tend to keep the grain size small. This is advantageous, as the flux pinning in Nb_3Sn is believed to be predominantly occurring by grain boundaries.[30,31,32] Also the filamentary form of Nb_3Sn enhances the pinning of fluxoids.

It is stated[33] that there is a critical thickness of the superconducting film below which there is a significant increase in H_{c2}. This critical thickness given by $d_c = \frac{2(\xi)^2\lambda}{K(t)}$. For Nb_3Sn, λ = 2900Å and K = 34. Thus d_c = 380Å. Although by the present fabrication technique such a thin film can be formed by quenching after reacting for a few seconds, the question remains, whether such a thin film network would be continuous.

D. Potential of the Composite as a Practical Superconductor

The feasibility of continuous fabrication into the final form is perhaps the most attractive feature. Perhaps an inert environment such as argon can used during sintering. Also operating the system with argon would be a good economical consideration compared to a vacuum system. The possibility of operating with a short cycle time - sintering taking 1/2 a minute, infiltration 1 minute, and heat treatment 3 minutes is another economical factor. Moreover continuity of the process would simplify the production management greatly.

As for the superconducting properties, the composite has critical temperature and critical currents characteristic of Nb_3Sn, and it is stable and flexible.

ACKNOWLEDGEMENTS

The author gratefully acknowledges the helpful suggestions and encouragement given from time to time during the progress of his work by Professors E. R. Parker and V. F. Zackay and the able guidance throughout by Dr. M. Pickus. Heartfelt gratitudes are due to John Holthuis, for the great assistance in the fabrication of samples and his keen interest in the work. Also, many thanks to Ferd Voelker and Bill Acker for their assistance in making steady-field measurements. Thanks are also due to Prof. R. M. Fulrath for his kind assistance in powder classification.

This work has been done under the auspices of the United States Atomic Energy Commission through the Inorganic Materials Research Division of the Lawrence Berkeley Laboratory.

APPENDIX A.

CYYSTAL STRUCTURE AND PROPERTIES OF Nb-Sn COMPOUNDS

Phase	Crystal Structure	Lattice Parameters a	b	c	T_c	H_c
$NbSn_2$	Orthorombic	9.838	5.644	19.215[18]	1.89 - 2,65°K[18]	620G (T=0°K)[34]
Nb_6Sn_5	Orthorombic	5.66	9.114	16.993	1.6 - 2.68°K[18,35,36]	500-600G(T=2.1°K)[36]
Nb_3Sn	β-Tungsten	5.282-5.29 for 18 at.% - 26 at.%[18]			18.5°K	220 KG (T=4.2°K)

REFERENCES

1. J. E. Kunzler, El Buchler, F. S. L. Hsù and J. H. Wernick, Phys. Rev. Letters 6, (3), 89 (1961).
2. Information sheet issued by RCA, Harrison, N.J.
3. M. G. Benz, 'Superconducting Properties of Diffusion Processed Nb-Sn Tape', IEEE Trans on Magnetics Vol. MAG-2, No. 4, Dec. 66. Also from an information sheet issued by GE, Schenectady, N.Y.
4. This technique is being patented by the laboratory in the names of Dr. M. Pickus, Prof. Parker and Prof. Zackay.
5. T. Garret, M. S. Thesis, to be published.
6. L-L. Wyman, J. R. Cuthill, G. A. Moore, J. J. Park and H. Yakowitz. J. of Research of the National Bureau of Standards-A. Physics and Chemistry. Vol. 66A, No. 4, July-Aug 62.
7. Alfred Seeger, Trans of Met-Soc.. AIME, 2987-2996, Vol-I, Nov. 70.
8. T. D. Livingston, GE Report Aug. 68.
9. R. R. Hake, Appl Phys. Letters, 10, 189 (1967).
10. U. Essmann and H. Trauble, Phys. Letters, 27A, 156 (1968).
11. H. Trauble and U. Essmann, J. Appl. Phys. 39, (1968).
12. C. P. Bean, Phys. Rev. Letters, 8, 250 (1962). Rev. Mod. Phys. 36, 31 (1964).
13. H. London, Phys. Letters 6, 162 (1963).
14. K. J. Gifkins, C. Malseed and W. A. Rachinger. Scripta Met. 2, 141 (1968).
15. The roll assembly design was by Dr. M. Pickus.

16. M. L. Picklesimer, U.S.A.E.C, Oak Ridge Natl. Lab. Rept 2296, (1957).

17. R. Enstrom, T. Courtney, G. Pearsall, and J. Wulff. Met of Adv. Elec. materials, edited by G. E. Brock, 121 (1962).

18. J. P. Charlesworth, I. Macphall, P. E. Madsen, J. of Mat. Sciences 5 580 (1970).

19. T. B. Reed, H. C. Gatos, W. J. Lafeur, and J. T. Roddy, Met. of Adv. Electronic Materials, edited by G. E. Brock, (1962) 71-86.

20. Ferd Voelker, PP 205-207, Particle Accelators, Vol. I, (1970).

21. M. Suenaga and K. M. Ralls, J. of Appl. Phy., 37, No. II, 4197 (1966).

22. H. J. Bode and Y. Uzel, Phys. Letters 24A, No. 3, 141 (1967).

23. J. J. Hanak, K. Strater and G. W. Cullen, RCA-report 25, 342 (1964).

24. T. H. Courtney, G. W. Pearsall and J. Wulff, Trans. of Met. Society-AIME, P212 (1965).

25. G. Rassmann, P. Muller and G. Hufnagel, Phys. Stat. Sol (a) 2, K105 (1970).

26. P. F. Smith, 'A Guide to Superdonductivity' edited by D. Fishlock (1969) P66.

27. T. H. Alden, and J. D. Livingston, App. Phys. Letters 8 (I), 6, (1966).

28. R. Hecht, RCA Review, (Sept. 1964) 453.

29. C. F. Old, I. Macphail, J. of Materials Science 4, 202 (1969).

30. A. R. Kaufmann, J. J. Pickett, Bulletin of Am. Phys. Soc. 15, 838 (1970).

31. E. Nemback and T. Tachikawa, J. of the Less Common Metals, 19, 359 (1969).

32. J. S. Caslaw, P57-59, Cryogenics, Feb. 71.

33. R. J. Duffy and H. Meissner, Phys. Review 147, (I), 248, (1966).

34. D. J. Van Ooijen, J. H. N. Van Vucht and W. F. Druyvesteyn, Phys. Letts 3, No. 3, (1962).

35. T. G. Ellis, H. A. Wilhelm, J. of Less Common Metals 7, 67 (1964).

36. R. E. Enstrom, J. of Appl. Phys. 37, No. 13, (1966).

FIGURE CAPTIONS

Note: Phase Identification in photomicrographs:

White: Tin, Light Gray: Niobium, Dark Gray: Nb_3Sn.

Fig. 1(a). Edge C. S.* of 'as infiltrated' sample made with -270 mesh powder 440x.

(b) Center C. S. of the same sample made with -270 mesh powder 440x.

Fig. 2. Center C. S. of 'as infiltrated' sample made with -500 + 750 mesh powder 440x.

Fig. 3. Center C. S. of 'as infiltrated' sample made with -750 + 1000 mesh powder 440x.

Fig. 4. Center C. S. of 'as infiltrated' sample made with -1000 mesh powder 440x.

Fig. 5(a). L. S.** of infiltrated and 50% rolled sample made with -270 mesh powder 440x.

(b). L. S. of infiltrated and 75% rolled sample made with -270 mesh powder 440x.

(c). L. S. of infiltrated and 85% rolled sample made with -270 mesh powder 440x.

(d). L. S. of infiltrated and 95% rolled sample made with -270 mesh powder 440x.

(e). L. S. of infiltrated and 75% rolled sample made with -750 + 1000 mesh fraction of Nb powder.

---

* C. S: Cross Section

** Longitudinal Section.

Fig. 6(a). Scanning Electron Micrograph of -500 + 750 mesh powder 250x.

(b). Scanning Electron Micrograph of -750 + 1000 mesh powder 250x.

(c). Scanning Electron Micrograph of -1000 mesh powder 250x.

Fig. 7(a). Photograph of the Rolling Mill Assembly.

(b). Photograph of the ABAR furnace set up for the infiltration of the sample.

Fig. 8. Correlation of the amount of tin squeezing out with the degree of cold work.

Fig. 9(a). Edge C. S. of 'as infiltrated' sample, made with -270 mesh powder, and reacted for 16 hours at 1000°C. 440x.

(b). Center C. S. of the same sample. 440x.

Fig. 10. C. S. of Specimen No. JC-1 680x.

Fig. 11. C. S. of Specimen No. JC-2 680x.

Fig. 12. L. S. of Specimen No. JC-3 680x.

Fig. 13(a). L. S. of Specimen No. JC-4 680x.

(b). L. S. of Specimen, 81% reduced, reacted for 2 mts. in Helium at 1200°C.

Fig. 14. Equilibrium Diagram of Nb-Sn system.[18]

Fig. 15. Schematic of the circuitry used for transition temperature measurement.

(a). Sample Connections.

(b). Theronister Connections.

Fig. 16. Variation of Transition Temperature with the Reaction Temperature for times of heat treatment, varying from a few minutes to one hour.

Fig. 17. Resistivities of sample JC-3 for different current densities at different d.c. fields.

Fig. 18. Short Sample Characteristic giving the current densities for different fields, for Samples JC-1, JC-2 and JC-3.

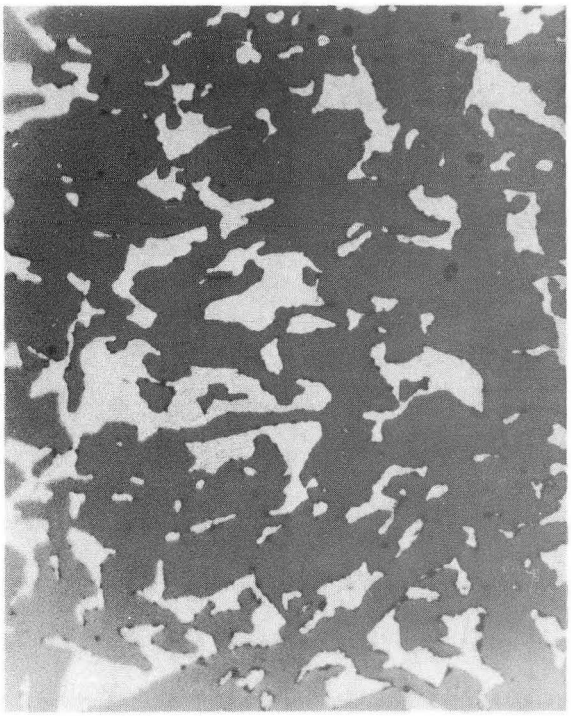

440x

Fig. 1(a)

440x

Fig. 1(b)

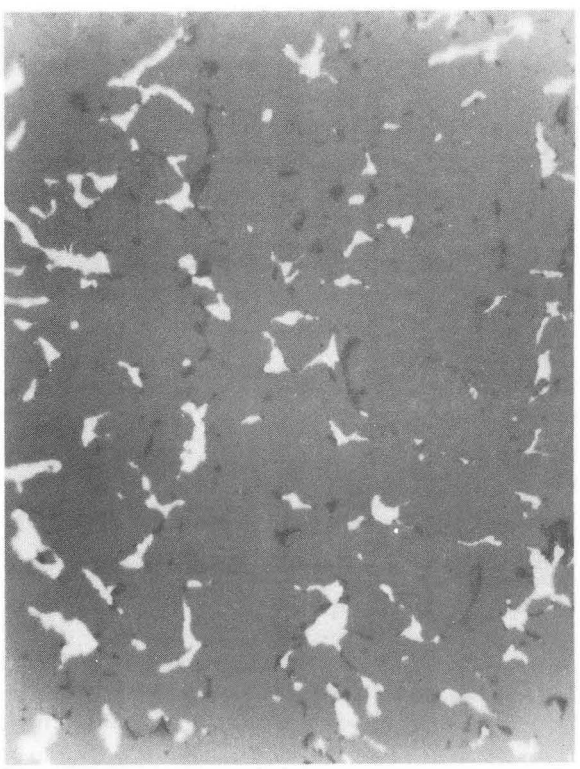

440x XBB 7112-5783

Fig. 2.

440x

Fig. 3.

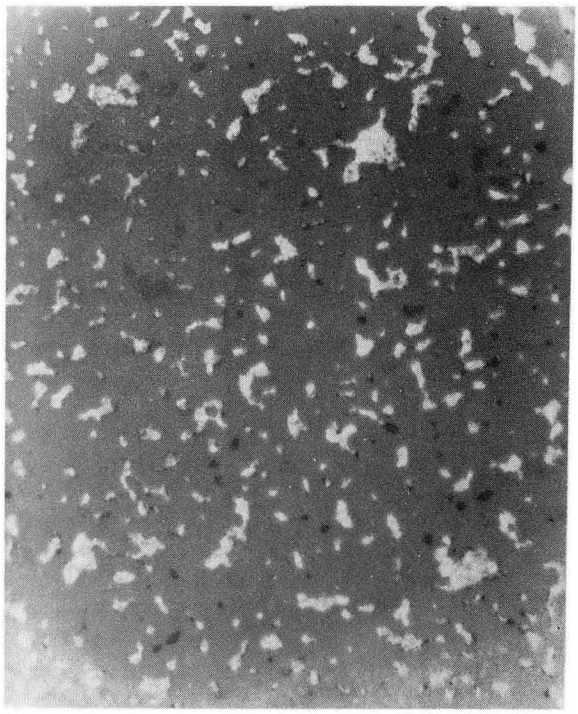

440x

Fig. 4.

440x XBB 7112-5786

Fig. 5(a).

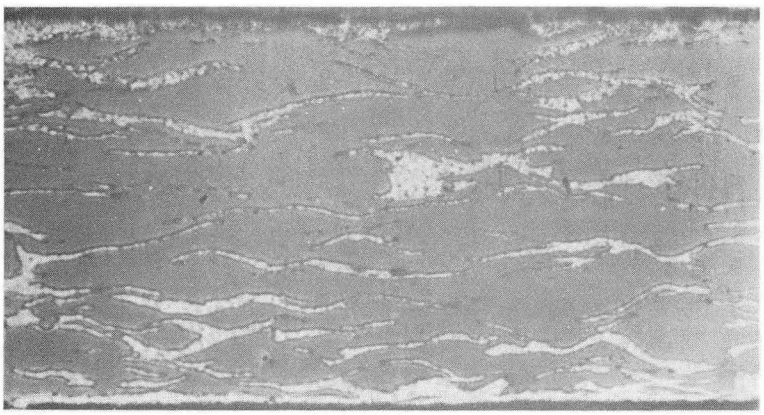

440x

Fig. 5(b)

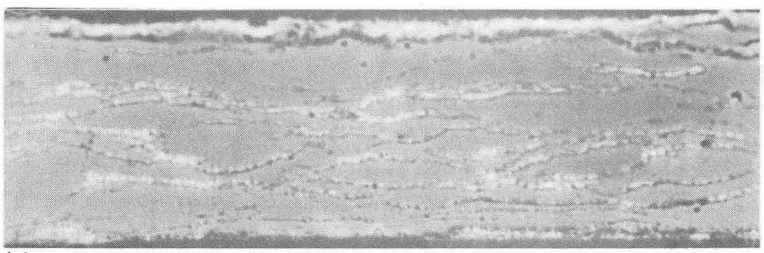

440x

Fig. 5(c)

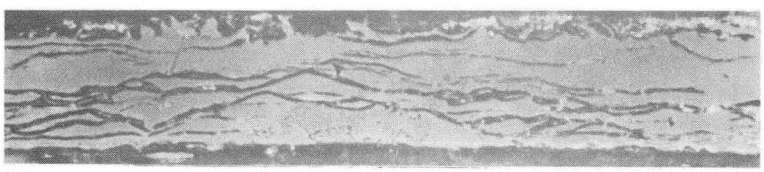

440x

Fig. 5(d)

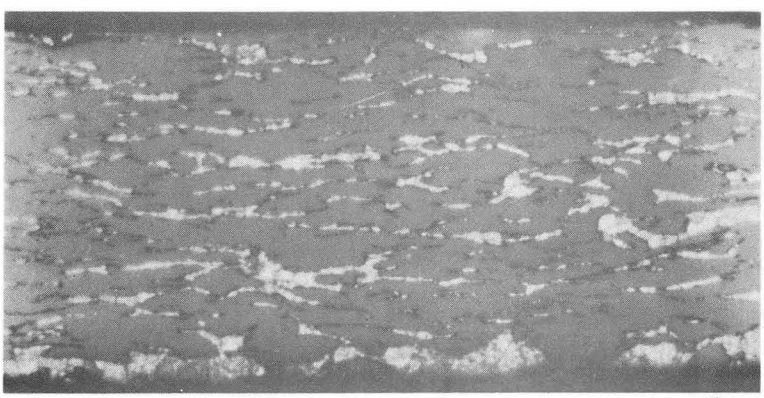

440x XBB 7112-5785

Fig. 5(e)

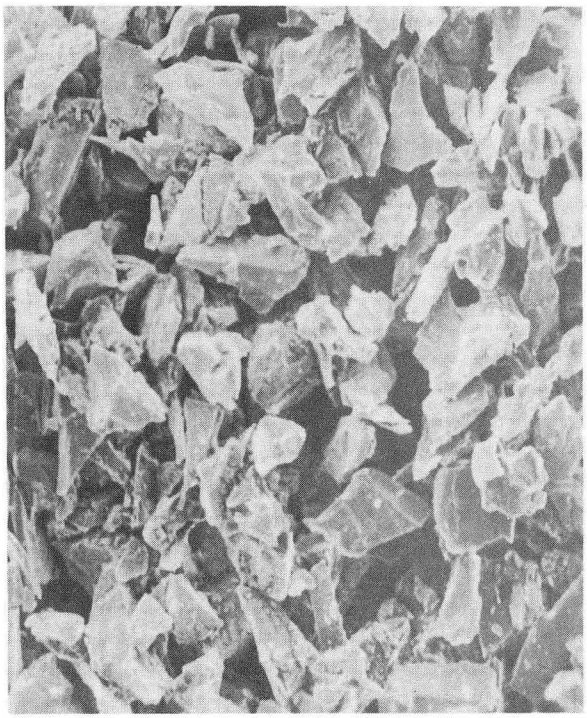

250x

Fig. 6(a)

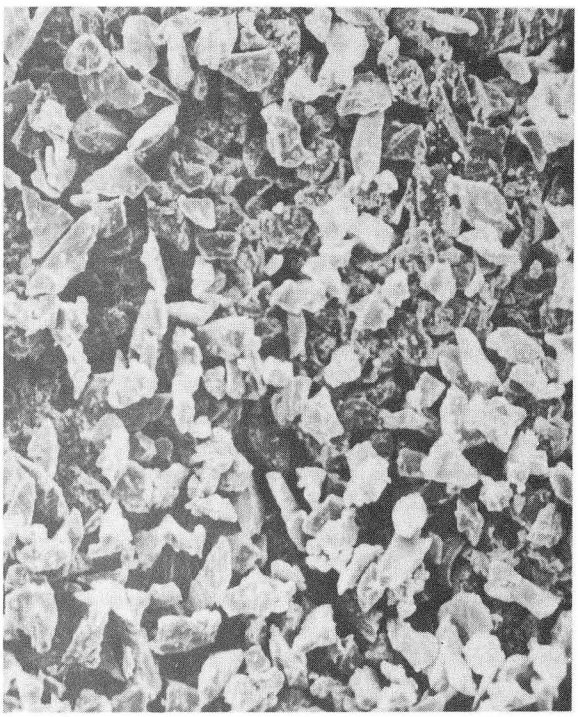

250x

Fig. 6(b)

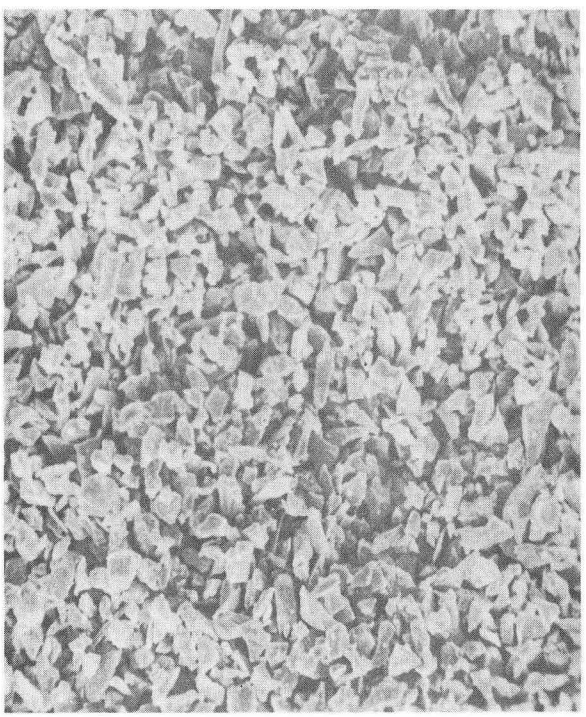

250x XBB 7112-5782

Fig. 6(c)

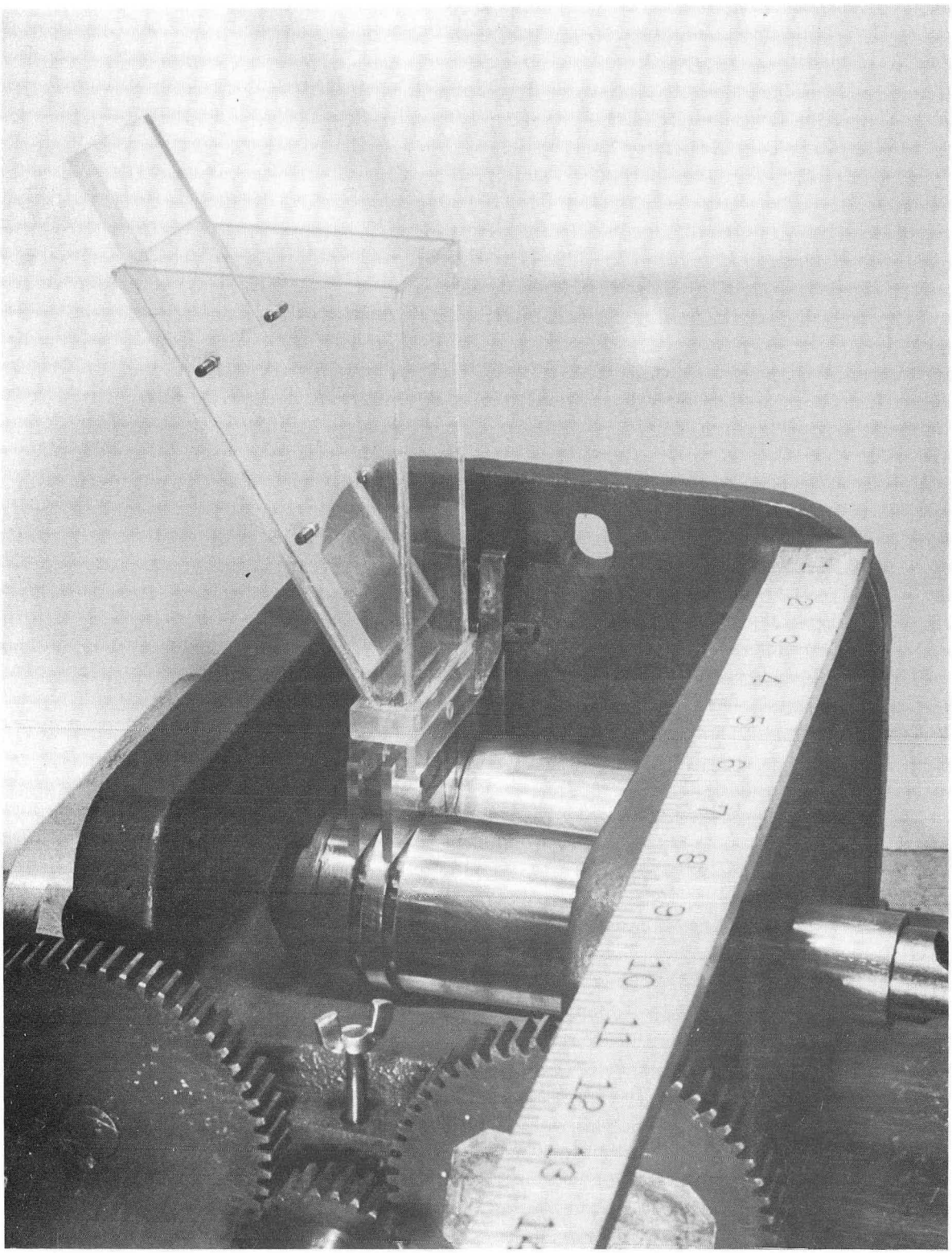

XBB 7011-5225

Fig. 7(a).

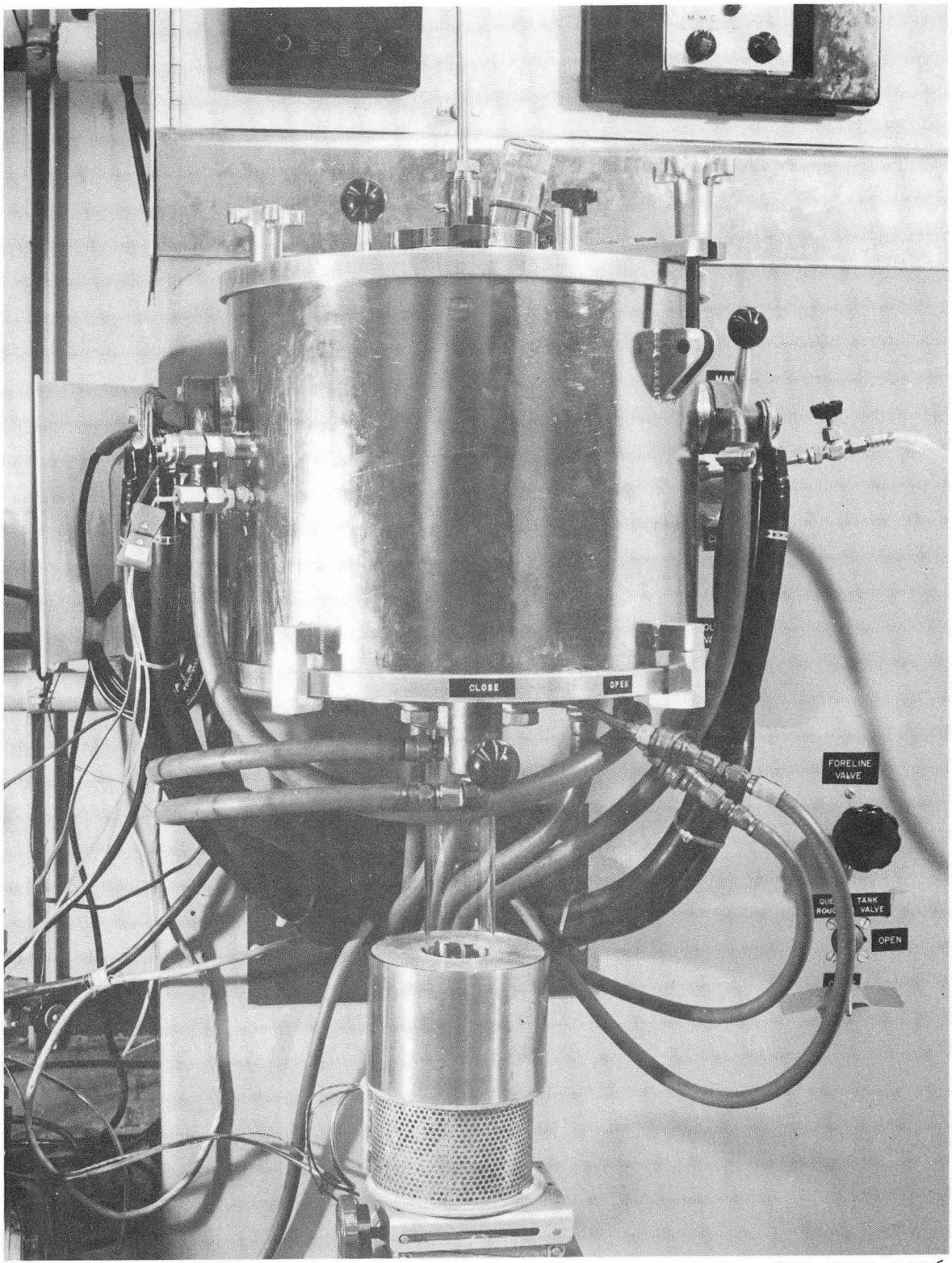

XBB 7011-5226

Fig. 7(b).

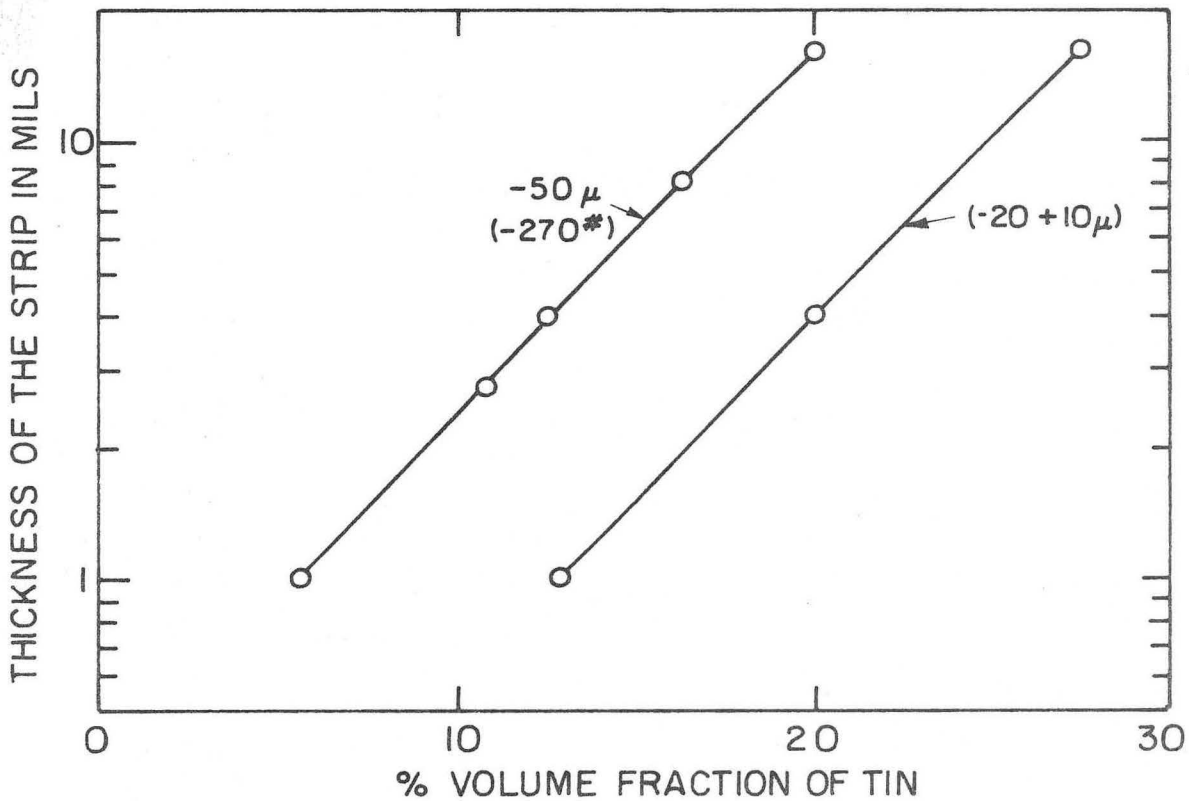
THICKNESS OF THE STRIP IN MILS
10
1
-50 μ
(-270#)
(-20 +10μ)
0
10
20
30
% VOLUME FRACTION OF TIN
XBL 7110-7516

Fig. 8.

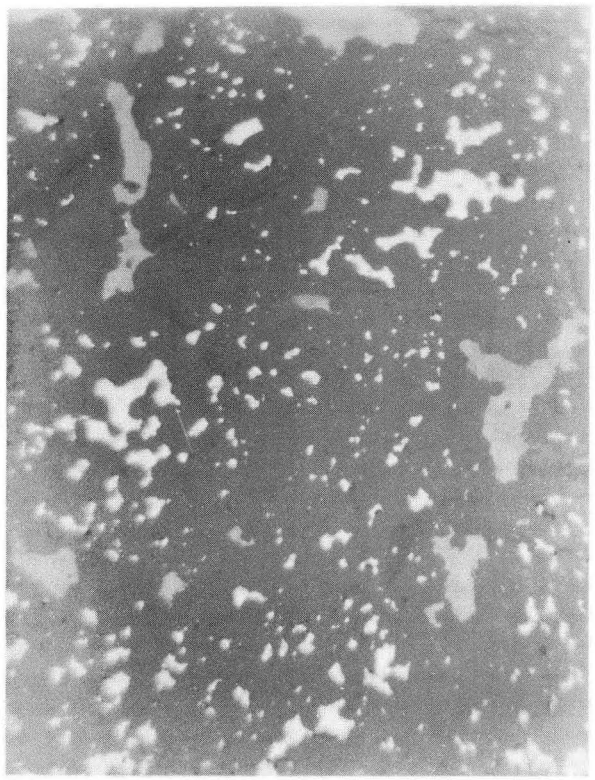

440x

Fig. 9(a).

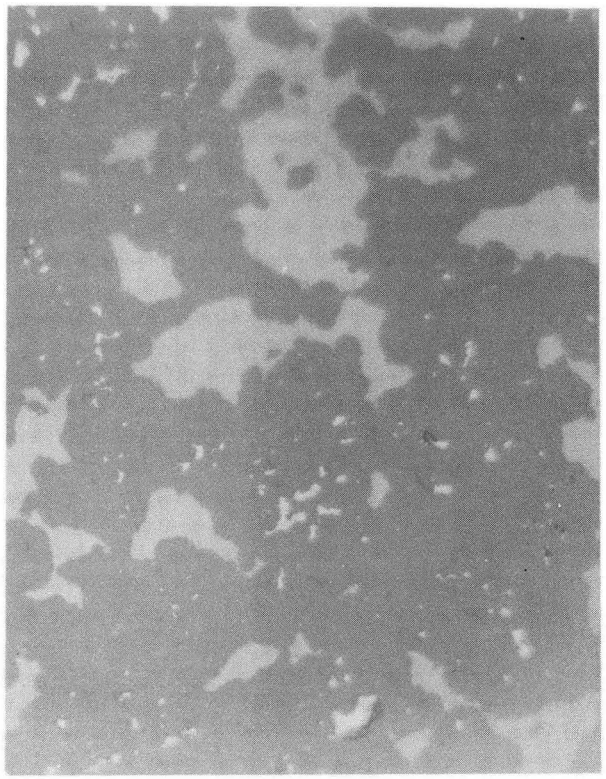

440x

Fig. 9(b).

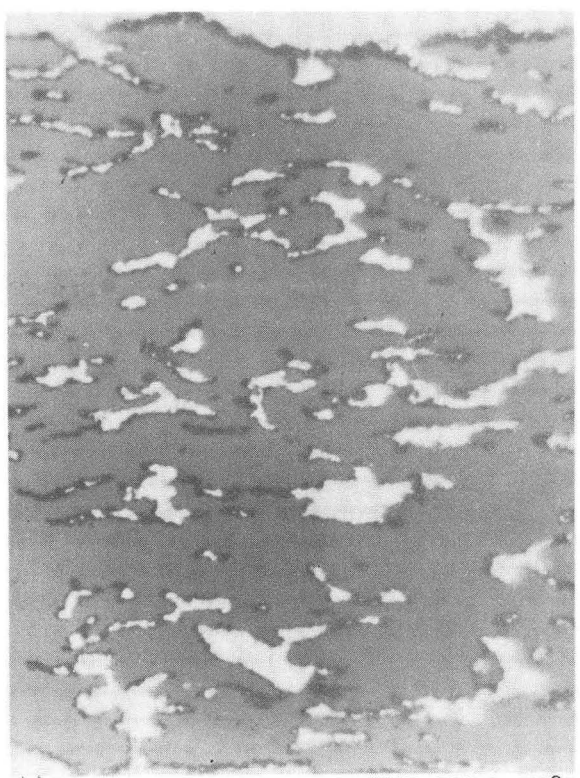

440x XBB 7112-5781

Fig. 10.

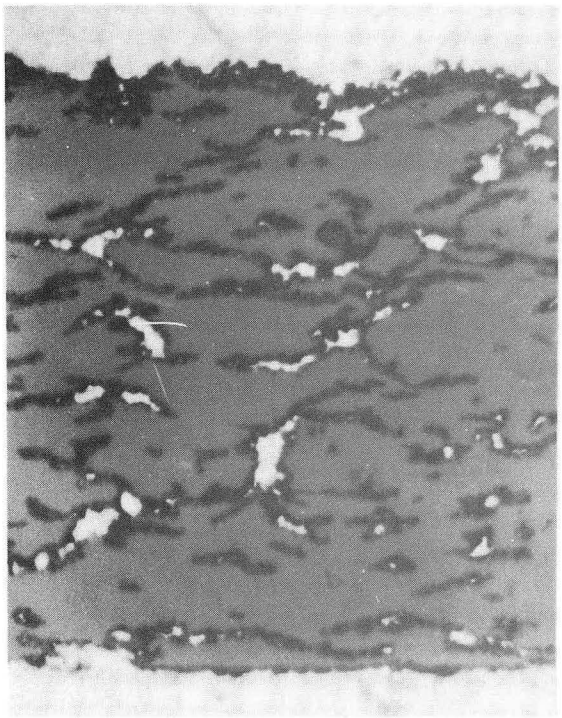

680x

Fig. 11.

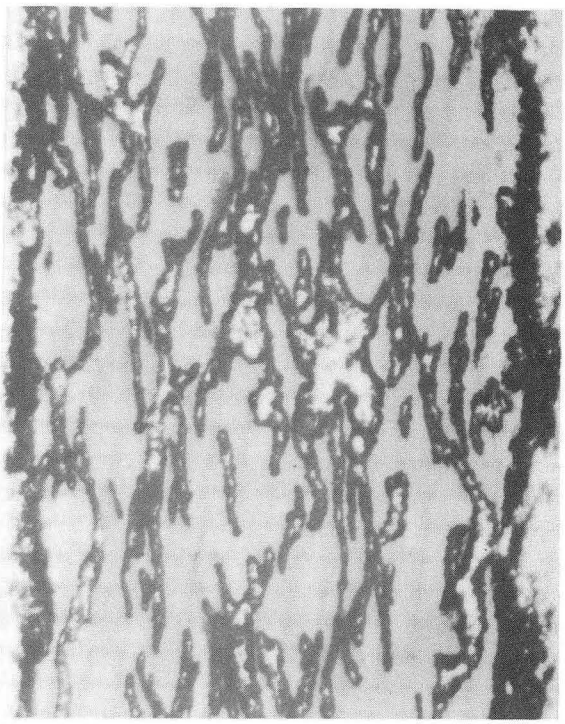

680x

Fig. 12.

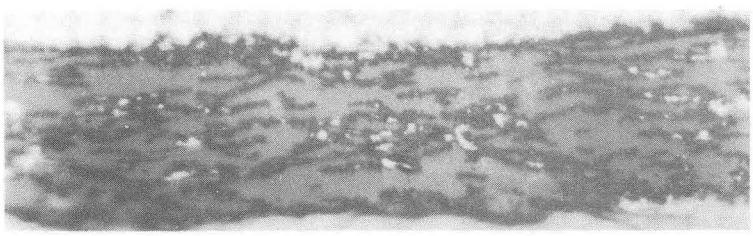

680x

Fig. 13(a).

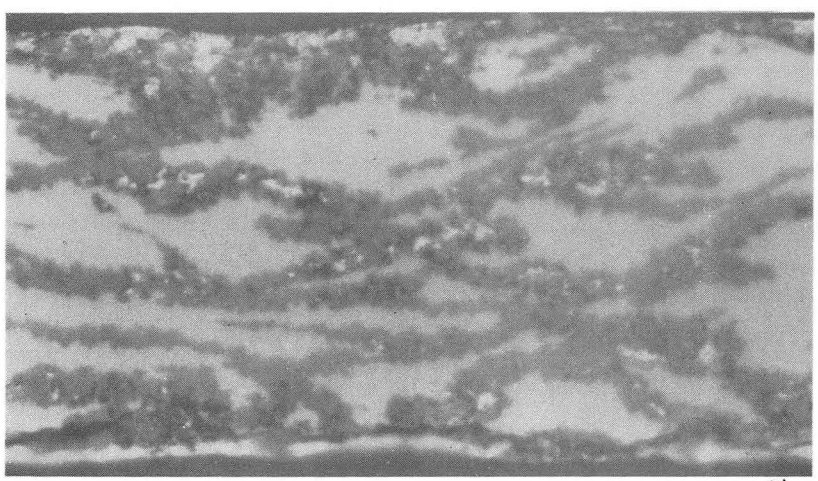

680x

XBB 7112-5784

Fig. 13(b).

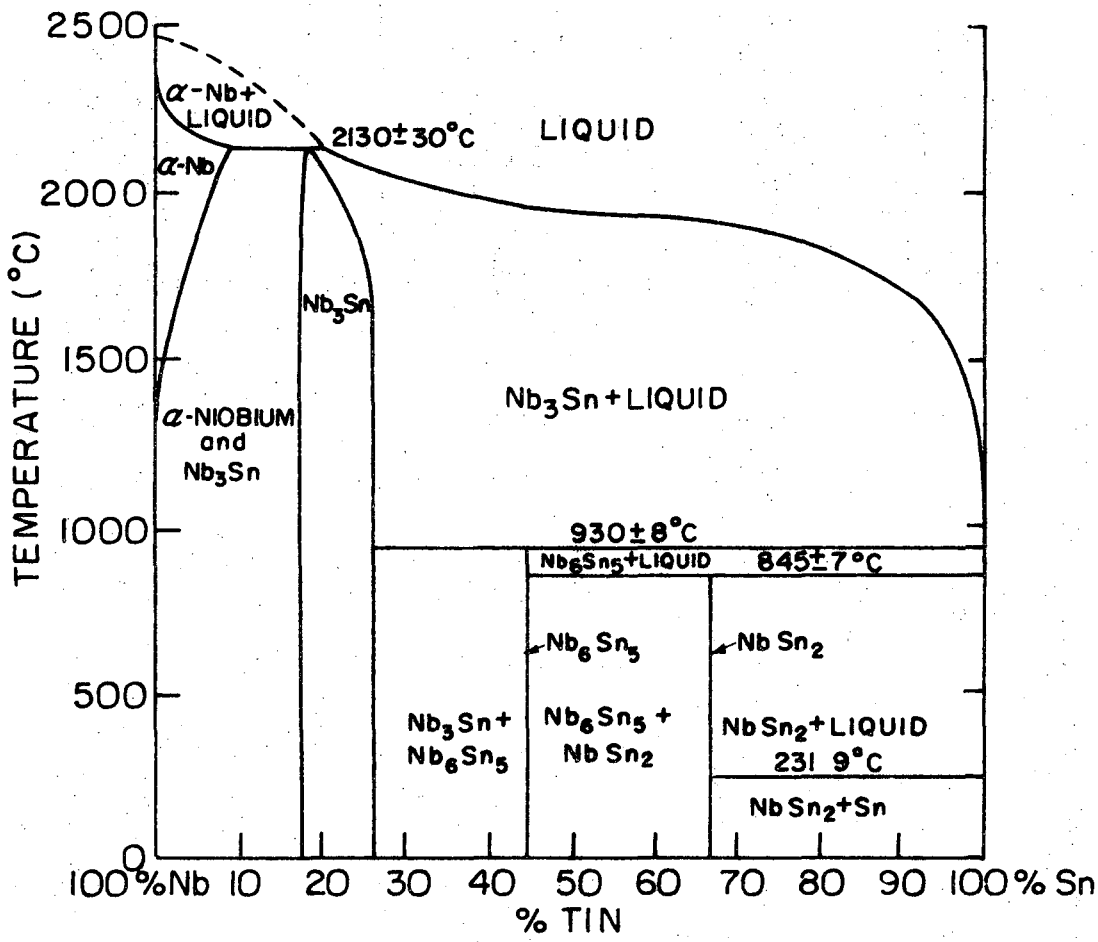

XBL 7110-7515

Fig. 14.

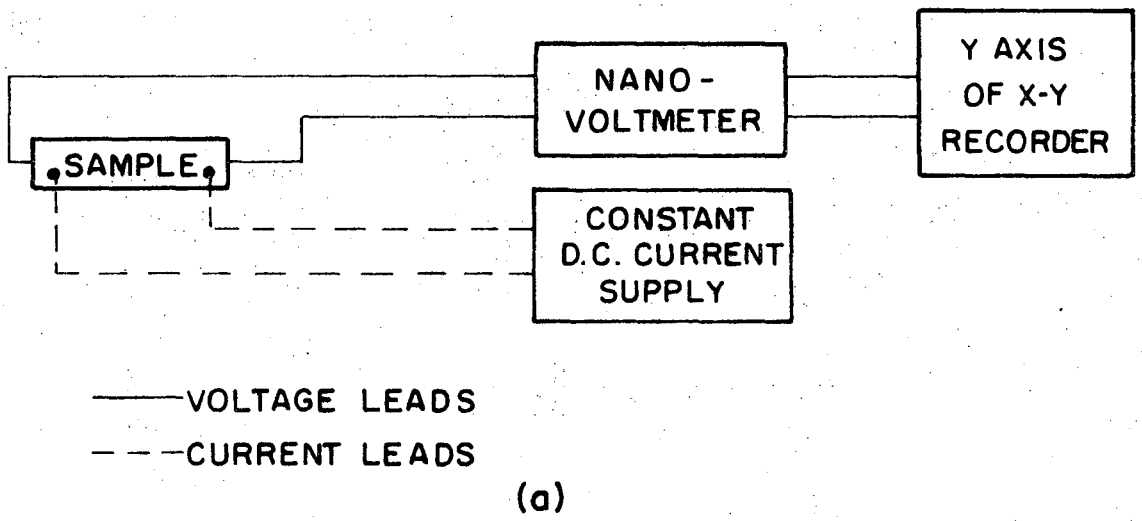

(a)

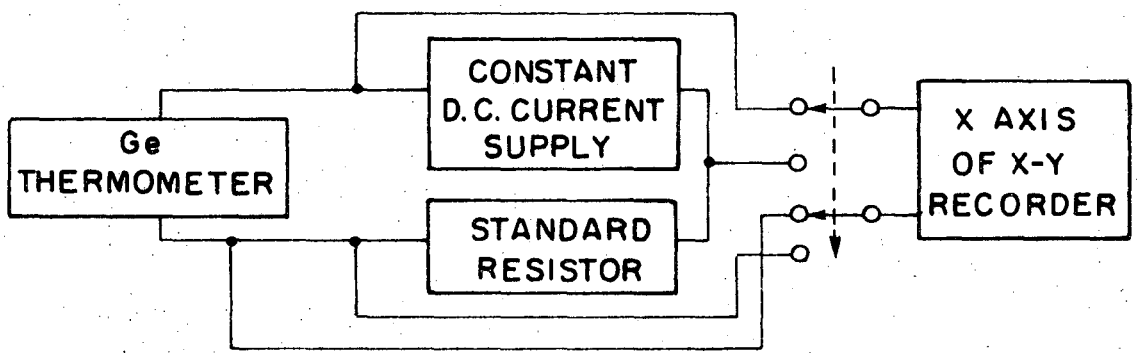

(b)

XBL7110-7428

Fig. 15.

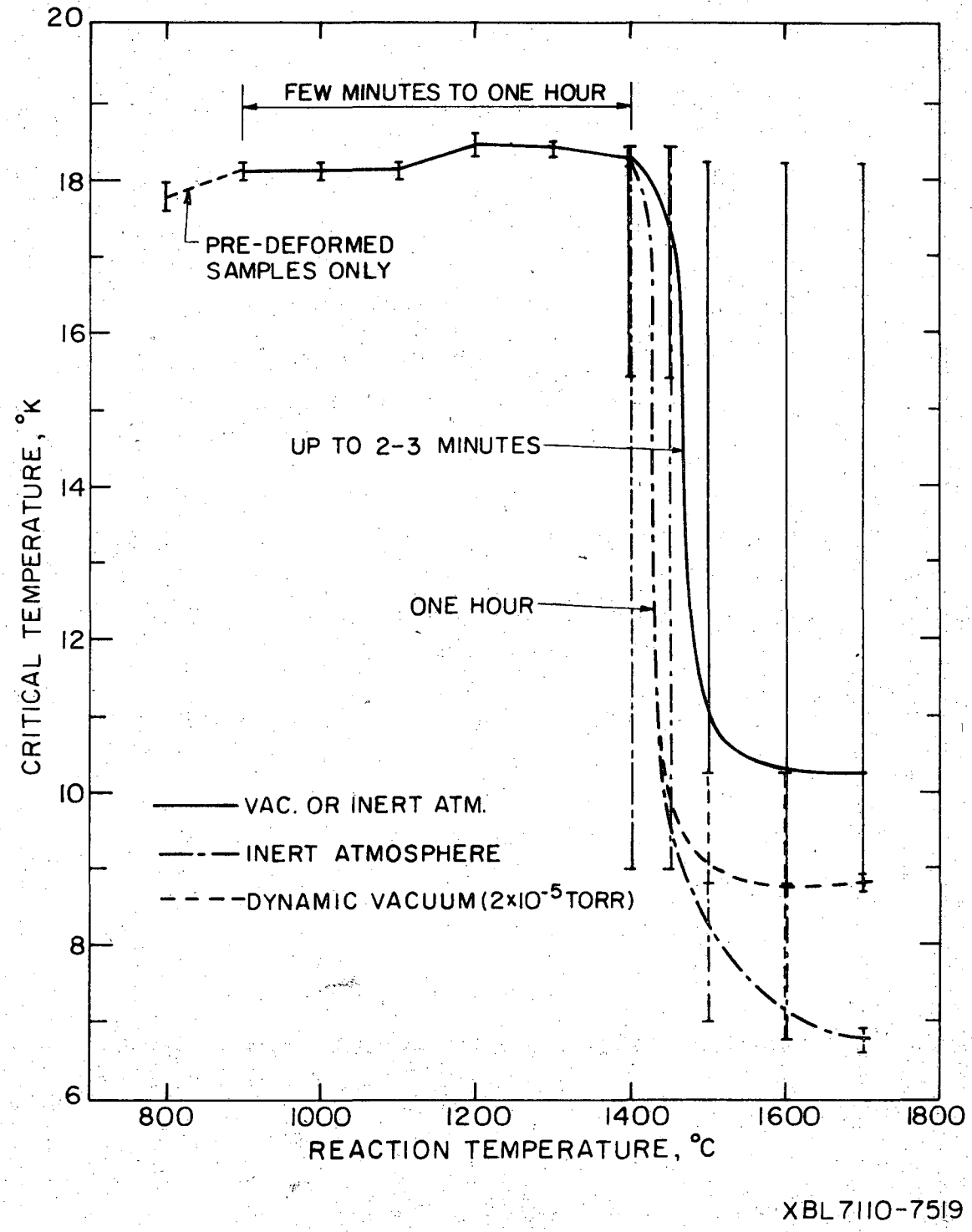
FEW MINUTES TO ONE HOUR
PRE-DEFORMED SAMPLES ONLY
UP TO 2-3 MINUTES
ONE HOUR
VAC. OR INERT ATM.
INERT ATMOSPHERE
DYNAMIC VACUUM (2×10⁻⁵ TORR)
CRITICAL TEMPERATURE, °K
REACTION TEMPERATURE, °C
20
18
16
14
12
10
8
6
800
1000
1200
1400
1600
1800
XBL7110-7519

Fig. 16.

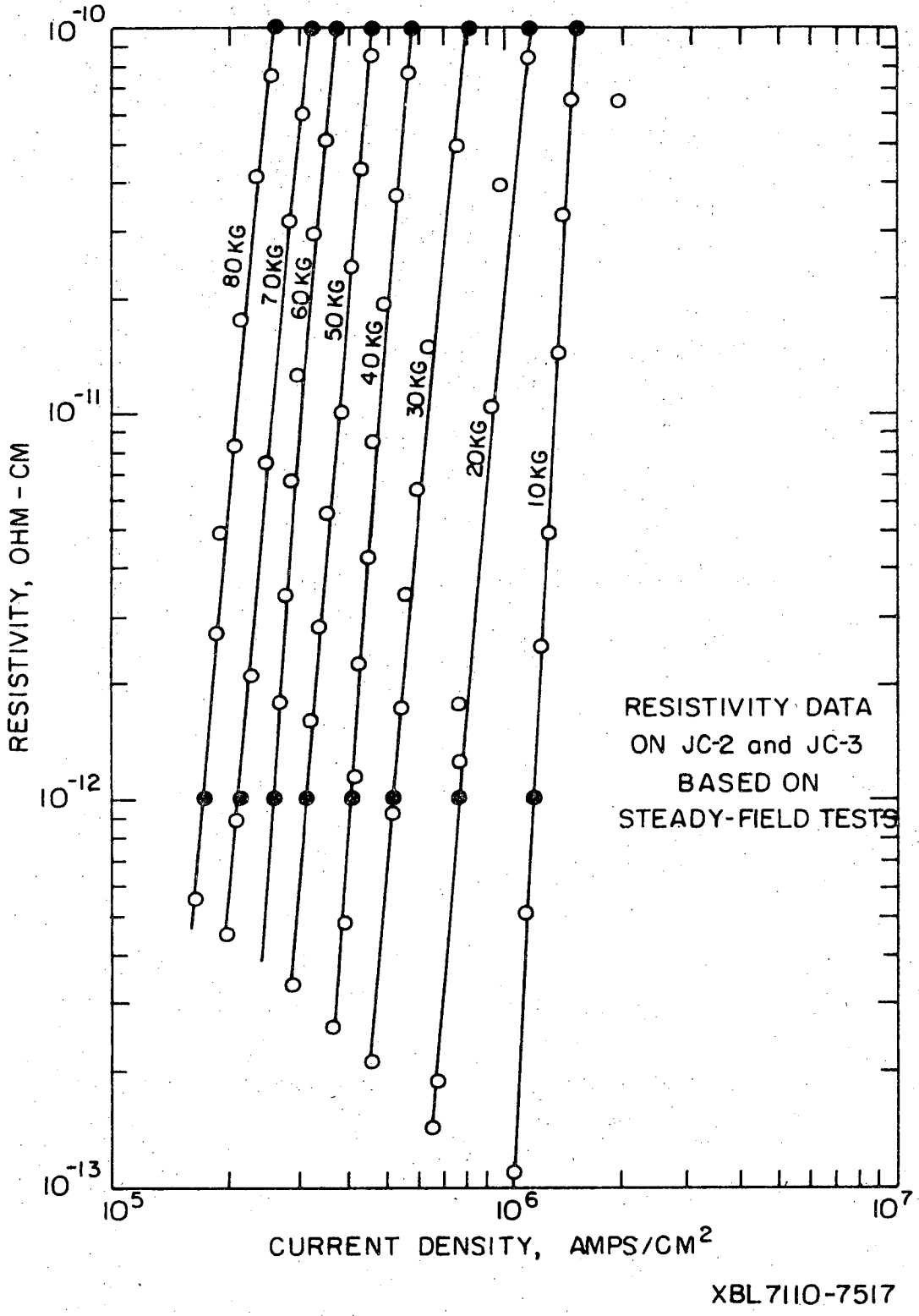
RESISTIVITY, OHM-CM
10^{-10}
10^{-11}
10^{-12}
10^{-13}
80 KG
70 KG
60 KG
50 KG
40 KG
30 KG
20 KG
10 KG
RESISTIVITY DATA
ON JC-2 and JC-3
BASED ON
STEADY-FIELD TESTS
10^5
10^6
10^7
CURRENT DENSITY, AMPS/CM^2
XBL7110-7517

Fig. 17.

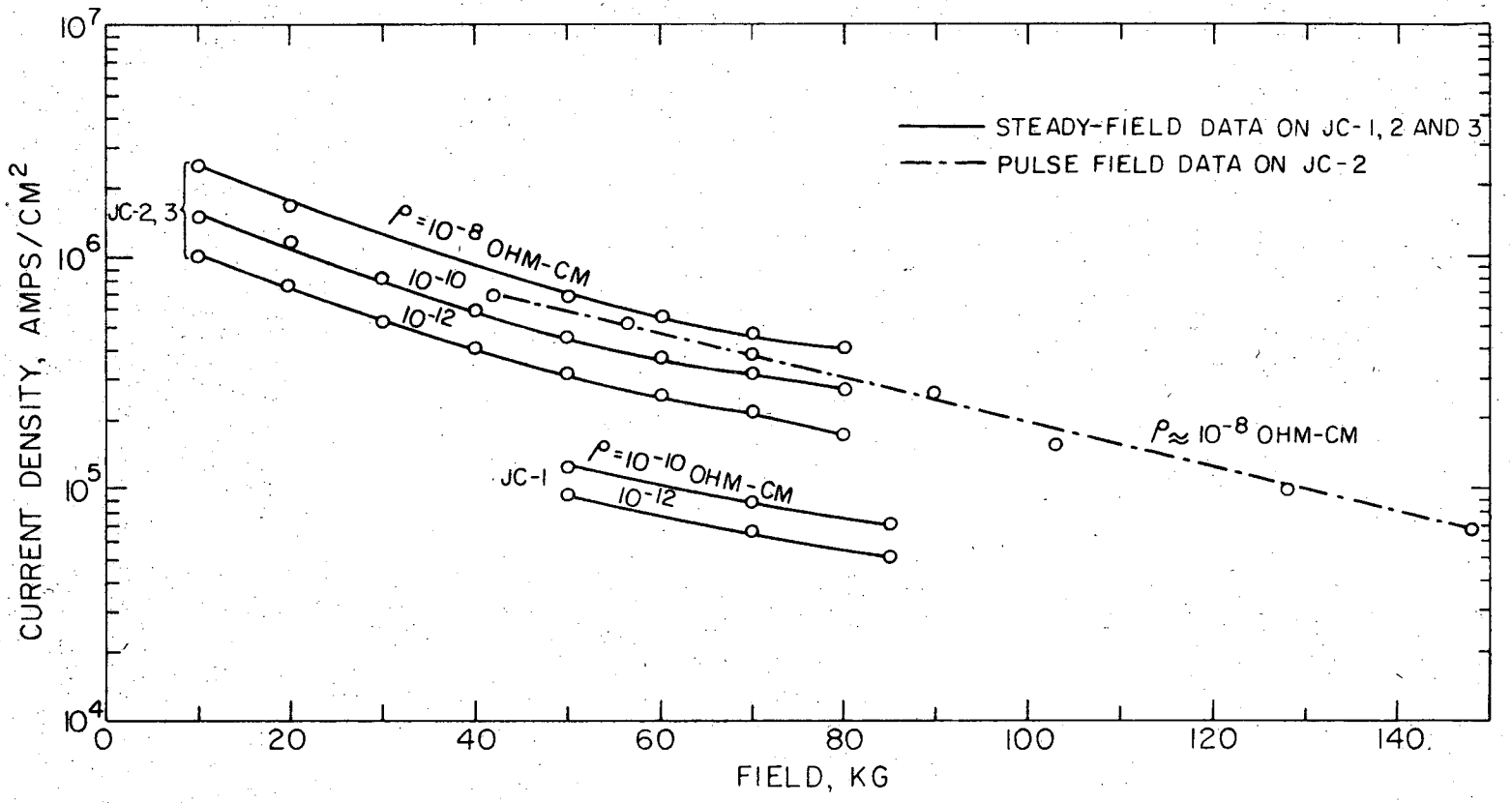

XBL 7110-7518

Fig. 18.

TECHNICAL INFORMATION DIVISION
LAWRENCE BERKELEY LABORATORY
UNIVERSITY OF CALIFORNIA
BERKELEY, CALIFORNIA 94720